The paper was presented at the Ninth Meeting
“New Trends in Fatigue and Fracture” (NT2F9)
Belgrade, Serbia, 12-14 October 2009

Donka Angelova, Rozina Yordanova, Dimiter Krasstev, Boyan Yordanov

COMPARISON OF BENDING AND ROTATING BENDING FATIGUE OF LOW-CARBON STEEL

POREĐENJE ZAMORA SAVIJANJEM I OBRTNIM SAVIJANJEM NISKOUGLJENIČNOG ČELIKA

Original scientific paper
UDC: 620.17:669.15-194
Paper received: 14.10.2009

Author's address:
University of Chemical Technology and Metallurgy – Sofia,
8 Kl. Ohridski, 1756 Sofia, Bulgaria, r.yordanova@uctm.edu

Keywords
- short fatigue crack
- low-carbon, low alloyed steel
- rotation-bending and pure-bending tests
- modelling
- fatigue life

Abstract

Growth of short cracks on smooth specimen is observed under different loadings in rotation-bending low-carbon, low alloyed steel, and pure-bending fatigue tests were additionally performed. Special features of interaction between the surface cracks and the microstructure of investigated steel are studied. A model is proposed for growth rate of surface cracks vs. their lengths by a system of parabolic and linear functions. Experimental results and models of both fatigue types are compared and some predictions are made, showing a reasonable agreement between the calculated by the model and experimentally obtained fatigue life.

Ključne reči
- kratka zamorna prslina
- nisko ugljenični niskolegirani čelik
- ispitivanje obrtnim savijanjem i čistim savijanjem
- modeliranje
- zamorni vek

Izvod

Rast kratkih prslina na glatkim epruvetama je praćen pri različitim opterećenjima u zamornom ispitivanju obrtnim savijanjem niskougljeničnog, niskolegiranog čelika i dodatno je izvedeno zamorno ispitivanje čistim savijanjem. Analizirani su specijalni oblici interakcije površinskih prslina i mikrostrukture ispitivanog čelika. Predložen je model koji prikazuje zavisnost brzine rasta površinske prsline i njene dužine u sistemu paraboličkih i linearnih funkcija. Eksperimentalni rezultati i modeli za oba tipa zamora su upoređeni i izvedene su procene, koje su pokazale prihvatljivu saglasnost veka procenjenog pomoću modela i eksperimentalno određenog zamornog veka.

INTRODUCTION

Fatigue investigations are carried out on a rolled low-carbon, low-alloyed steel. They are based on short fatigue crack growth and its monitoring by replication of surface crack propagation from initiation to failure, /1, 2/. Here, the investigations include short crack rotation-bending experiments /3, 4/ and length measurements of propagating crack on smooth hour-glass specimens. Some specimens had a layer of modified surface specially treated by electrical-discharge in electrolyte. Results of rotation-bending fatigue are compared with additionally obtained in pure bending of flat specimens without layers, /4-8/.

The models describing the short fatigue crack growth behaviour at rotation-bending and pure bending, based on our first pull-pull model /5/ are proposed, including parabolic-linear presentation of the three stages of short fatigue crack propagation, known as *microstructural short (MSFC)*, *physically small (PhSFC)* and *long fatigue crack (LFC)* growth, /4, 5/. New models use a coefficient correction considering the most dangerous crack growth rates for each of the stages. Substantial microstructural barriers d_1, d_2 are stage boundaries and make cracks slow down and stop are defined in /5/. The proposed model gives possibilities for predictions of fatigue life at different conditions concerning the tested steel and applied loading; also it allows analytical generalisations of fatigue behaviour for a given class of steels.

EXPERIMENTAL PROCEDURE

A rolled low-carbon, low-alloyed steel (RLCLAS), marked as 09Mn2 Steel (according to the Bulgarian Construction Steel Standard), used mostly for offshore applications and in shipbuilding, was subjected to rotation-bending fatigue, /3, 4/. Two groups of specimens were investigated: the specimens without layer, tested under two stress ranges, $\Delta\sigma$ = 620 and 580 MPa, and specimens with layer, exposed to $\Delta\sigma$ = 580 and 500 MPa; applying stress ratio R = –1, and the frequency 11 Hz.

The chemical composition of the steel and its mechanical characteristics are given in Table 1.

Table 1. Specification of class RLCLAS 09Mn2 steel.
Tabela 1. Specifikacija čelika klase RLCLAS 09Mn2

Chemical composition (Hemijski sastav), %									
C	Si	Mn	Cr	Ni	P	S	Cu	Al	As
0.09	0.28	1.63	0.05	0.04	0.017	0.026	0.13	0.12	0.014

Mechanical properties (Mehaničke osobine)				
Tensile strength	Proof strength	Cross section contraction	Hardness	Average grain size
σ_B, MPa	$\sigma_{0,2}$, MPa	ψ, %	HB, MPa	μ m
482	382	62.3	148	25.6

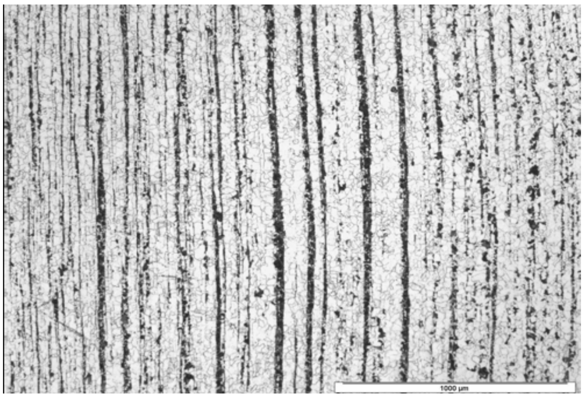

a.

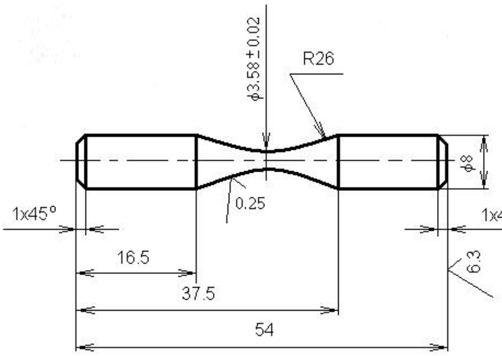

b.

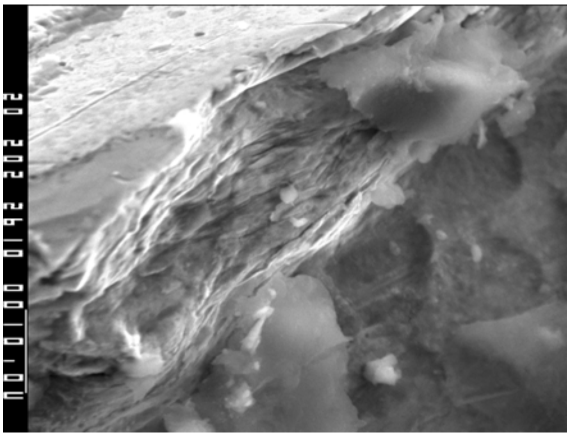
c.

Figure 1. Microstructure of cross section of RLCLAS steel (a), cylindrical fatigue specimen with dimensions in mm (b), microstructure of RLCLAS with a layer (c).
Slika 1. Mikrostruktura poprečnog preseka čelika RLCLAS (a), cilindrična epruveta za ispitivanje zamora, mere u mm (b), mikrostruktura RLCLAS sa slojem (c)

RLCLAS steel was available in sheets 8 mm thick. Its microstructure revealed a sequence of long and uniform pearlite and ferrite bands, as shown in Fig. 1a. The average ferrite grain size was d = 25.6 μm. The bands were wider in the middle of the sheet but loose and thinner close to the surface. Tests were carried out on a table model Fatigue Rotation-Bending Machine, Fatrobem-2004, /5/.

The specimens, (i) smooth hour-glass specimens without layer, and (ii) with a surface layer obtained at special conditions of electrical-discharge treatment in electrolyte, followed by high-speed cooling, are shown in Fig. 1b. At such conditions the surface layer is identified as having ultra-micro-crystal and nano-crystal structure, Fig. 1c.

The surface modified layer (here the specimen is subjected to 580 MPa) is produced with expectation for better weariness and longer fatigue lifetime. That is only a first attempt for fatigue testing of RLCLAS with such a layer and for modelling the obtained experimental results. There are some investigations of tool steels with a layer produced by the same technology, that show good results.

A third group of flat specimens is subjected to pure symmetric bending in air at stress range $\Delta\sigma$ = 580 MPa, stress ratio was R = –1 and frequency 5 Hz. Four micro-notches were milled by Focused-Ion-Beam (FIB) technique in different positions in the microstructure, /7/. Three of them were central (on longitudinal axis of specimen and perpendicular to it) and located in-between the pearlite bands; the fourth was an edge notch. The distance between notches was 200 μm.

Flat specimens, the notch geometry and sizes are given in Fig. 2.

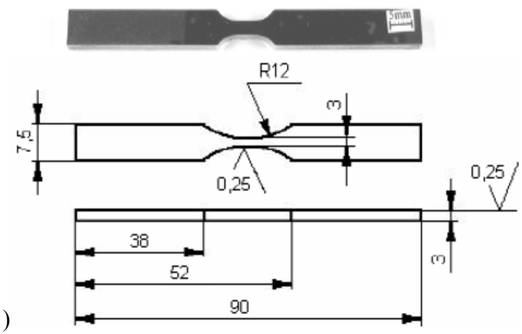

(2.1)

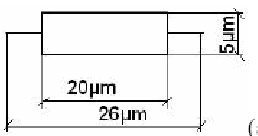

(2.2)

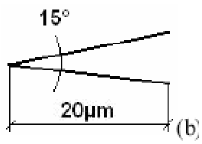

Figure 2. Flat fatigue specimen (dimensions in mm), 2.1, geometry of Focused Ion Beam (FIB)-notches in it, 2.2: central (a); edge (b).
Slika 2. Ravna epruveta za ispitivanje zamora (mere u mm), 2.1, geometrija FIB-zareza, 2.2: središnjeg (a) i ivičnog (b)

The surface short-crack propagation on cylindrical specimens during a fixed interval of fatigue cycles was monitored by acetate-foil replica technique and observed on the replicas by an optical microscope for measuring registered surface crack lengths. The short fatigue-crack experiments with flat specimens included interruptions of the test at every 1000 cycles for examination of the specimen surface under optical- or SEM-microscope. Crack lengths were measured by using an image analyser, /7/.

RESULTS AND DISCUSSION

Data obtained from rotating-bending and pure bending fatigue, crack lengths a (μm) and corresponding numbers of cycles N, are plotted in Fig. 3.

While Figs. 3a and 3b are plotted for well defined main cracks, in Fig. 3c are represented 4 cracks from 8 cracks all together, which have merged and led to final failure of flat-type specimens. In this case (described in detail in Ref. /6/) crack 1 started from the edge notch, bifurcated and one of the bifurcations propagated as crack 2, Fig. 4, that later merged with crack 3 that started from the central notch aligned with the edge notch. In this way the right part of the flat specimen had fractured at 39000 cycles. At the same time (39000 cycles) propagation of crack 4, Fig. 4, led to fracturing of the left part of the specimen and to its complete failure.

The approach adopted for modelling short fatigue crack propagation in its 3 stages – *SFC*, *PhSFC* and *LFC* – is described in /4, 6, 7, 8/ and the model in the present study is represented by parabolic-linear system of equations M, as given in Eqs. (1):

$$\text{M:}\quad \begin{aligned} &SFC\text{:} && \left(\frac{da}{dN}\right)_{sh} = A_1a^2 + A_2a + A_3; \quad a \in [a_0, d_1];\\ &PhSFC\text{:} && \left(\frac{da}{dN}\right)_{phs} = B_1a^2 + B_2a + B_3; \quad a \in [d_1, d_2]; \quad (1)\\ &LFC\text{:} && \left(\frac{da}{dN}\right)_{l} = C_1a^{C_2}; \quad a \ge d_2 \end{aligned}$$

where A, B, C are material constants (Table 2), d_1 and d_2 – microstructural barriers analytically determined as boundaries between the stages of *SFC*, *PhSFC* and *LFC* (Table 3) at which crack propagation is arrested and practically stops for some time, /6/.

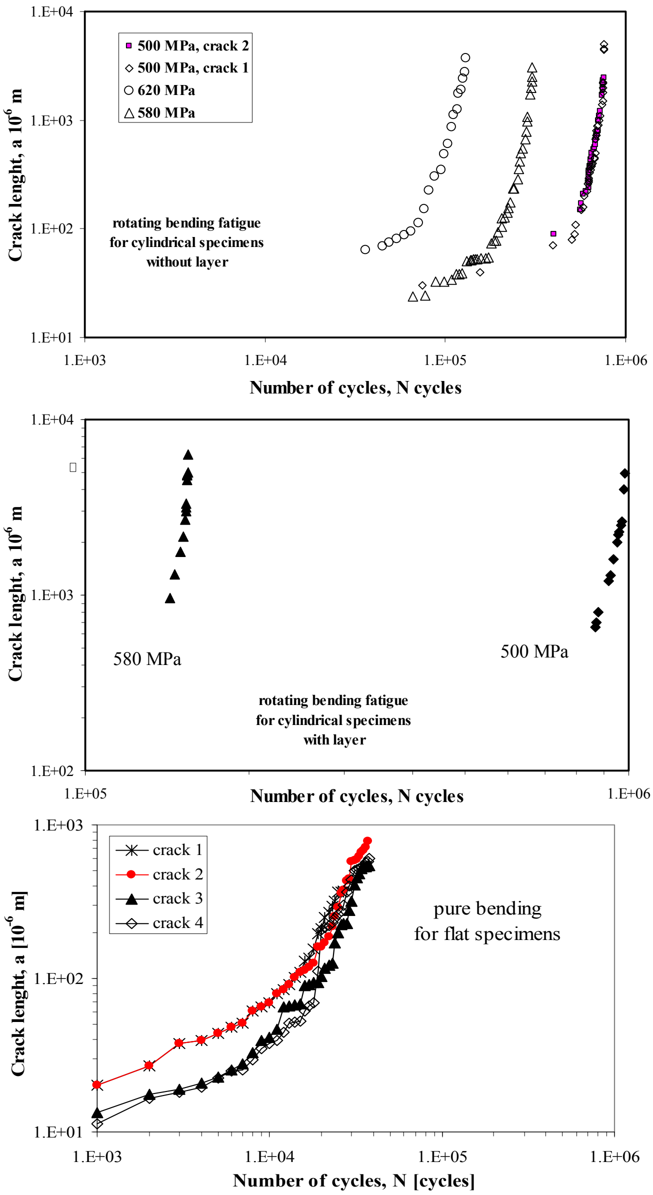

Figure 3. Plots of crack length, a vs. number of cycles, N at: rotating bending fatigue of cylindrical specimens, without layer (a), with layer (b); and pure bending for flat specimens (c).
Slika 3. Dijagrami dužina prsline a–broj ciklusa N, za obrtno savijanje cilindrične epruvete, bez sloja (a) i sa slojem (b), i za čisto savijanje ravne epruvete (c)

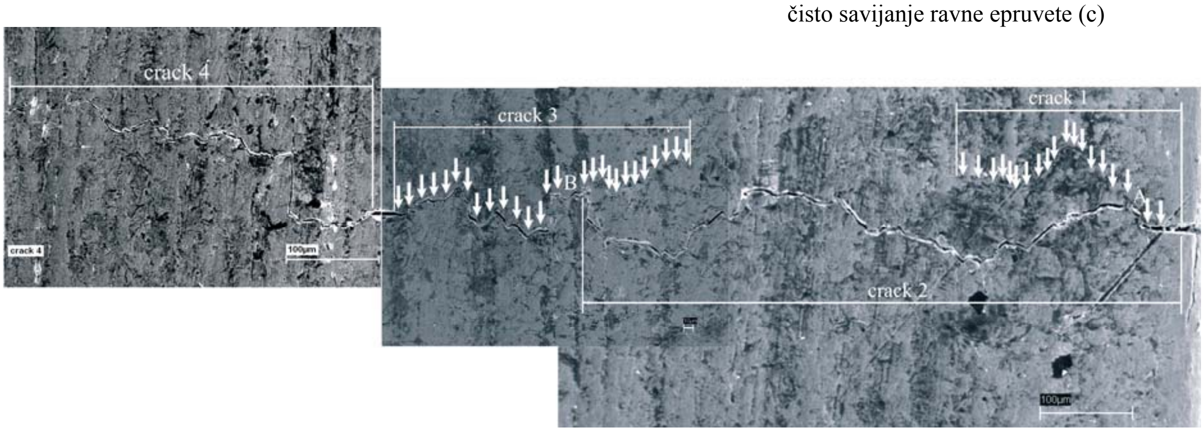

Figure 4. Flat specimen in its longitudinal axis: right part with cracks 1, 2, 3; and left part with crack 4.
Slika 4. Ravna epruveta gledana po uzdužnoj osi: desno deo sa prslinama 1, 2, 3; levo deo sa prslinom 4

Table 2. Coefficients A, B, C for some stress values at different experimental conditions.
Tabela 2. Koeficijenti A, B, C za neke vrednosti napona u različitim uslovima ispitivanja

$\Delta\sigma$, MPa	f, Hz	Short Crack			Physically Small Crack			Long Crack	
		A_1	A_2	A_3	B_1	B_2	B_3	C_1	C_2
ROLCLAS, cylindrical, without layer									
620	11	–	–	–	–0.00000047	0.000228	–0.0147	4.12×10^{-6}	1.3499
580		-1.4×10^{-6}	0.00014	–0.0022	-7.177×10^{-7}	0.000226	–0.0126	6.09×10^{-8}	1.944
ROLCLAS, cylindrical, with layer									
580	11	–	–	–	–	–	–	6×10^{-10}	2.6055
500		–	–	–	-1×10^{-7}	0.0002	–0.1046	2×10^{-9}	2.1815
ROLCLAS, flat specimen									
580	5								
crack 2		–0.0000012	0.000186	0.00374	–0.0000012	0.000907	–0.112986	2.32×10^{-21}	6.7310
crack 4		–0.00000255	0.00064	–0.01255	–0.0000016	0.00122	–0.18757	1.5×10^{-23}	7.6338

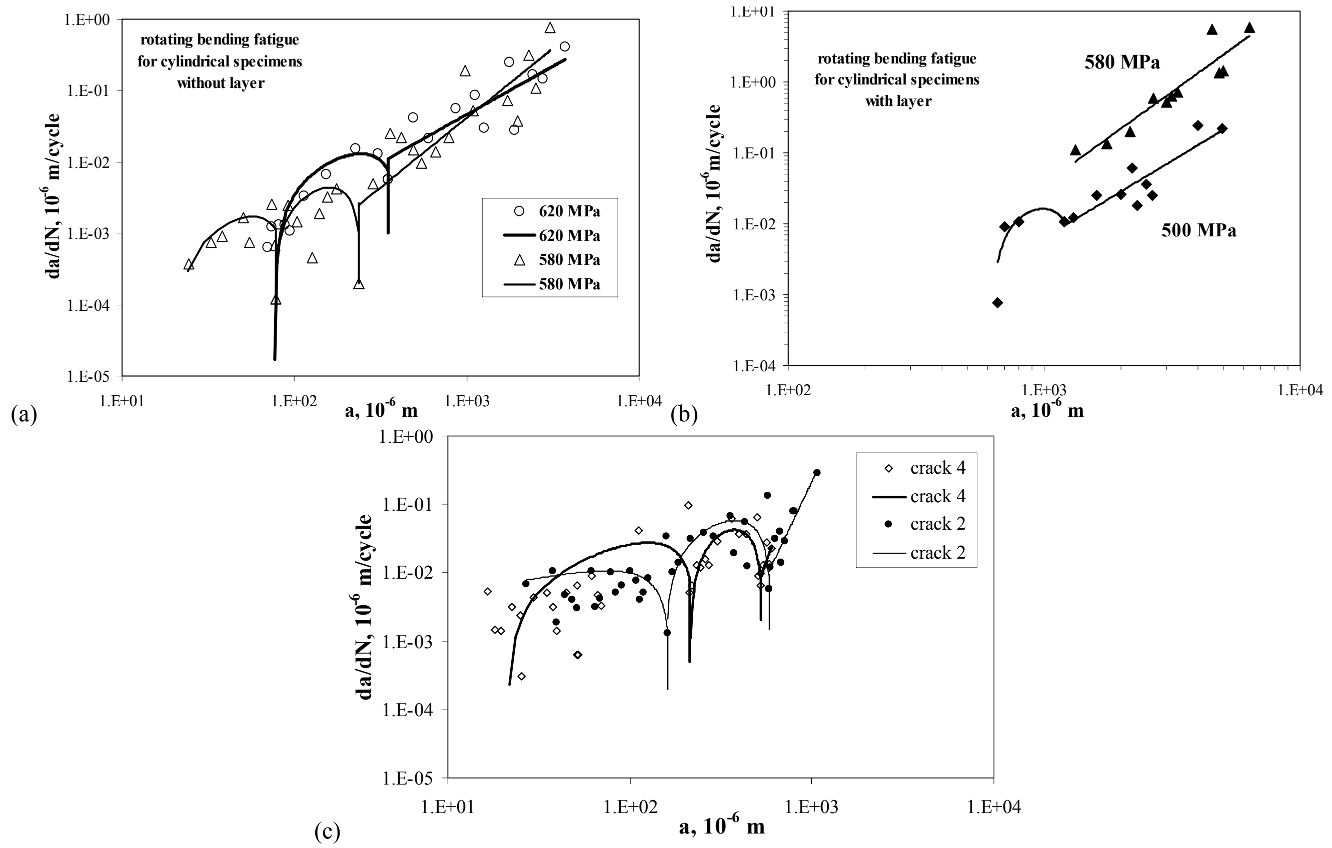

Figure 5. Plot of crack growth rate, *da/dN* vs. crack length *a*: rotation-bending fatigue, without (a) and with layer (b); (c) pure-bending fatigue.
Slika 5. Dijagrami brzina rasta prsline, *da/dN*–dužina prsline *a*: za obrtno savijanje cilindrične epruvete, bez sloja (a) i sa slojem (b), i za čisto savijanje ravne epruvete (c)

Table 3. Calculated by the model and experimentally obtained fatigue lifetimes.
Tabela 3. Zamorni vek, sračunat pomoću modela i dobijen eksperimentalno

Type of specimen	$\Delta\sigma$	a_0	a_f	d_1	d_2	N_0	$N_{f,exp}$	$N_{f,m}$	$100\times(N_{f,exp}-N_{f,m})/N_{f,m}$
ROLCLAS, cylindrical, without layer	580	24	3064	78	236	66018	304000	275940	9.23
	620	64	3705	94	348	36118	136398	130454	–4.55
ROLCLAS, cylindrical, without layer	580	–	6320	–	1200	143000	154550	149079	3.5
	500	–	4940	660	1200	866800	985490	1001784	–1.65
ROLCLAS, flat specimen, crack 2	580	17	603	161	583	2000	39000	45563	–16.8
crack 4		27	1079	213	526	2000	39000	45483	–16.8

$\Delta\sigma$–fatigue stress range; d_1–microstructural barrier; boundary between *SFC* and *PhSFC*; N_0–cycles to crack initiation; a_0–initial crack length; d_2–microstructural barrier, boundary between *PhSFC* and *LFC*; $N_{f,exp}$–experimental fatigue lifetime; a_f–final crack length; $N_{f,m}$–calculated fatigue lifetime

The model in its graphical form is represented in Figs. 5 and 6; it shows that pure bending with notched specimens is the most dangerous situation, Fig. 6. The proposed model is supported by the comparison of fatigue lifetimes from Eq. (2), $N_{f,m}$, and actual, $N_{f,exp}$, obtained in experiment, at primary cycles to crack initiation, $N_{f,0}$. To estimate the applicability of the proposed model, values of $N_{f,m}$ and $N_{f,exp}$ are compared for some stresses, Table 3.

$$N_{f,m} = N_{f0} + \int_{a_0}^{d_1} \frac{da}{L_{shc}(A_{shc}a^2 + B_{shc}a + C_{shc})} + \int_{d_1}^{d_2} \frac{da}{L_{psc}(A_{psc}a^2 + B_{psc}a + C_{psc})} + \int_{d_2}^{a_f} \frac{da}{L_{lc}A_{lc}a^{B_{lc}}} \quad (2)$$

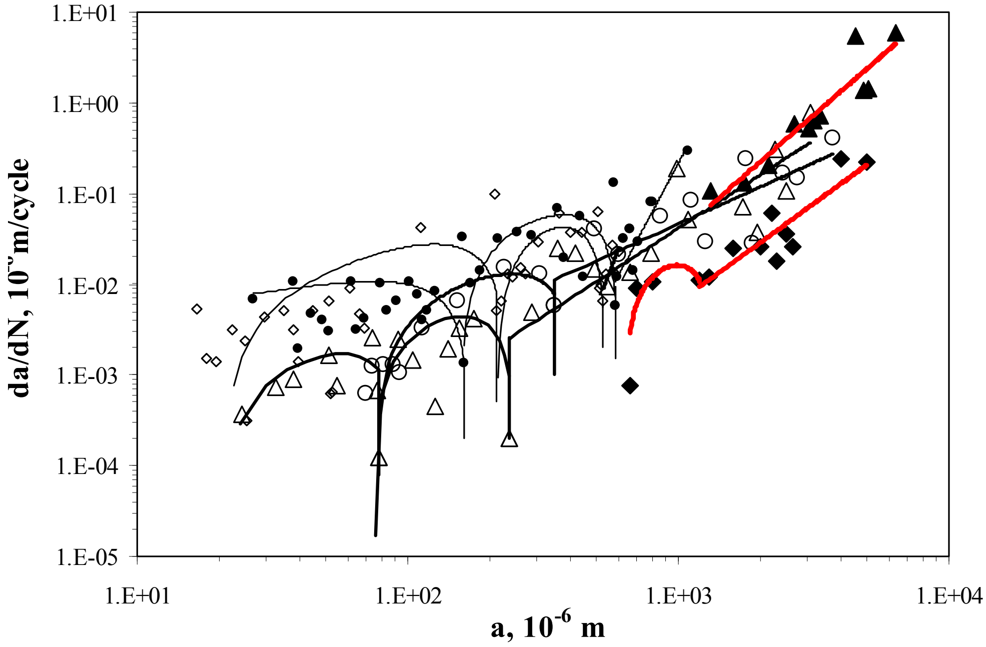

Figure 6. Plot of crack growth rate *da/dN* vs. crack length *a,* combination of all graphs from Fig. 5.
Slika 6. Dijagram brzina rasta prsline *da/dN*–dužina prsline *a*: kombinacija svih dijagrama sa sl. 5

SUMMARY

Two groups of cylindrical specimens of a low-carbon steel without and with a modified surface layer are subjected to rotation bending fatigue. Specimens with the modified surface layer show higher crack growth rates and longer cracks for shorter fatigue life in comparison with the specimens without layers. More experience is needed considering the usual large scatter in fatigue data.

A third group of flat specimens of the same steel are preliminary notched by FIB-technique alongside their longitudinal axis and at one of the edges, and then subjected to pure bending fatigue in terms to analyse interaction between the surface cracks and the microstructure. The obtained data show higher crack growth rates (dominated by the interaction with ferrite and pearlite grain boundaries and interfaces, ferrite grains, pearlite colonies and non-metal inclusions) and shorter fatigue life in comparison with the specimens subjected to rotation bending fatigue. Crack propagation rates decrease in the vicinity of (i) interface between ferrite and pearlite bands when a crack propagates into the ferrite or pearlite colony, and (ii) ferrite-ferrite or pearlite-pearlite grain boundary, (iii) obstacles, where a crack changes its propagation direction or bifurcates. Rows of longitudinal nonmetallic inclusions (MnS) increase crack growth rate, serving as crack paths.

The proposed Parabolic-linear model can describe and predict adequately short crack behaviour under rotation-bending and pure-bending fatigue. This is additionally supported by comparison of predicted and actual fatigue lifetimes.

ACKNOWLEDGEMENTS

The authors thank the University of Chemical Technology and Metallurgy, Bulgaria, for its valuable support on Contracts 10637, 10638.

REFERENCES

1. Suresh, S., *Fatigue of Materials*. Cambridge Univ. Press, Cambridge, UK, 1998.
2. Miller, K.J., *The three thresholds for fatigue crack propagation*, Fatigue Mechanics: 27th Volume, ASTM STP 1296, pp.267-286, 1997.
3. Yordanova, R., Angelova, D., Naydenova, Z., Stoyanova-Ivanova, A., Mikli, V., *Rotating-bending fatigue in a low-carbon steel*, Structural Integrity and Life, Vol.10, No2, 2010, pp.89-94.
4. Angelova, D., Davidkov, A., *Different analytical presentations of short crack growth under rotation-bending fatigue*, Proceedings 16th European Conference on Fracture, Failure Analysis of Nano and Engineering Materials and Structures, pp.175-176, Alexandropoulos, Greece, 2006.
5. Davidkov, A., Yordanova, R., *Comparative analyses on the fatigue behaviour of low carbon steel at different loading in laboratory air*, Journal of the UCTM, Sofia, vol.XXXVIII, 4 (2003), pp.1177-1184, 2002.
6. Davidkov, A., On factors influencing fatigue in 09Mn2 steel, PhD Thesis, University of Chemical Technology and Metallurgy – Sofia (UCTM) (in Bulgarian), 2007.
7. Davidkov, A., Pippan, R., *Studies on short fatigue crack propagation through a ferrite-pearlite microstructure*, Book of Abstracts O135, 9th International Fatigue Congress, Atlanta, Georgia, USA, 2006.
8. Yordanova, R., Modelling of fracture process in a low-carbon 09Mn2 steel on the bases of short fatigue crack growth experiments. PhD Thesis, UCTM, 2003.